

Angular Correlations between Characteristic L X Rays and Scattered α Particles

J. Konrad, R. Schuch, and R. Hoffmann

Physikalisches Institut Universität Heidelberg, D-6900 Heidelberg, Federal Republic of Germany

and

H. Schmidt-Böcking

*Physikalisches Institut Universität Heidelberg, D-6900 Heidelberg, Federal Republic of Germany, and
Institut für Kernphysik, D-6000 Frankfurt/Main, Federal Republic of Germany*

(Received 13 September 1983)

From the complete angular correlation between the L x rays and scattered α particles after ionization of the Dy L_{III} subshell by 16-MeV α particles, the impact-parameter-dependent A_{20} , A_{22} , and A_{21} alignment tensor components were determined. These alignment tensor components which characterize the magnetic substate ionization and the relative phases between the ionization amplitudes are in reasonable agreement with semi-classical-approximation predictions.

PACS numbers: 34.50.Hc

The alignment of the L_{III} subshell induced by collisions with charged particles has attracted steadily increasing interest in recent years. In an ion-atom collision process a quantization axis (z axis) may be provided by a perturbation of the spherical symmetry of the target atom by the Coulomb field of the ionizing projectile. This causes a spatial distribution of the different angular momentum states with respect to such a quantization axis and thus different ionization probabilities for the different magnetic substates (alignment) in the collision process. The alignment of the target atom after the collision can be determined by studying its subsequent decay by characteristic x-ray or Auger-electron emission.^{1,2} From a nonisotropic angular distribution of the L_i x rays ($3s_{1/2}-2p_{3/2}$ transition) in coincidence with scattered particles we were able to extract the impact-parameter dependence of the A_{20} , A_{22} , and A_{21} alignment tensor components, and of course also the ionization probability of the L_{III} subshell. This is almost the greatest degree of information about the ionization process of an atomic shell with total angular momentum $j \geq \frac{3}{2}$ that can be obtained from an angular distribution measurement.

Most of the previous experimental studies of alignment of inner-shell ionization³⁻⁵ were done without coincidence with the scattered particles. From such experiments, which represent an average over all impact parameters and are axial symmetric along the beam direction, only an average A_{20} tensor component can be extracted. These values, which correspond to the difference in the total ionization cross sections of magnetic substates with $|m_j| = \frac{3}{2}$ or $|m_j| = \frac{1}{2}$, were meas-

ured³⁻⁵ as a function of the projectile energy. As regards this dependence, the data were found to be in reasonable agreement with the predictions of first-order perturbation theory [plane-wave Born approximation, semiclassical approximation (SCA)].

In this Letter we report the first measurement of the impact-parameter dependence of A_{20} , A_{22} , and A_{21} alignment tensor components of the L_{III} subshell of heavy target atoms induced by light-ion bombardment. These alignment tensor components were determined for collisions of 16-MeV α particles on Dy from the measured angular distribution of the L_i x rays detected in coincidence with scattered α particles. Besides our experiment, one other coincidence measurement for inner-shell alignment, induced, however, by electron collisions, has been made.⁶ There, an incomplete angular distribution of the $L_3-M_{23}M_{23}$ Auger electrons emitted only in the scattering plane at two different scattering angles was measured. From these results only two correlation parameters were derived and the alignment tensor components could not be determined.

In our experiment a well collimated 16-MeV α -particle beam from the EN tandem accelerator at Max Planck Institut für Kernphysik, Heidelberg hit a Dy target. The x rays were detected with four Si(Li) detectors mounted in one plane at four different polar angles θ (25° , 38° , 90° , and 100°) with respect to the beam direction. The energy resolution of the Si(Li) detector at $\theta = 38^\circ$ was $\cong 240$ eV (full width at half maximum) and for the other three Si(Li) detectors it was better than 190 eV (full width at half maximum) at 5.9 keV. The scattered particles were detect-

ed with a radial and azimuthal position-sensitive, avalanche detector (PPAD).⁷ The particle detector consisted of two detector layers; the one with radial resolution was divided into fourteen concentric rings and the detector with azimuthal resolution was divided into sixteen sectors.

By a coincidence requirement between the detected x rays and the signal of the radial position-sensitive detector, we measured the photon emission probabilities as a function of the impact parameter b . By requiring an additional coincidence condition between the radial and the azimuthal position-sensitive detectors in the PPAD, we simultaneously determined the impact parameter and scattering plane of the scattered projectiles in coincidence with the detected L x rays. Thereby $14 \times 16 \times 4$ different particle scattering angles with respect to the direction of photon emission were measured simultaneously.

During the experiment the total L x-ray rate in each Si(Li) detector was typically on the order of 50 Hz, whereas the detected-particle rate varied between 0.1 and 0.5 MHz depending on the scattering angle. The ratio of true-to-random coincidences varied between 2:1 and 4:1. The procedure of data reduction is described by Hoffmann *et al.*⁸ The background in the x-ray energy spectra, for which the data were corrected, amounted to $\approx 30\%$ of the L_I intensity in the window of the L_I line. In order to determine the solid-angle ratios between the different Si(Li) detectors we used the isotropic K radiation of a Mn target without coincidence requirement. Additionally, the coincidences with the L_γ and L_α lines were used to test the setup for any other possible apparatus anisotropy, because the L_γ line should be emitted isotropically and the L_α line should have only a small anisotropy of about 5% at 100% alignment. Indeed, for the L_γ and L_α lines we found no anisotropy in the dependence on b , nor either the polar or azimuthal photon emission angles, as would be expected for a setup with no anisotropy.

The measured anisotropies of the L_I line have to be corrected for an isotropic contribution from Coster-Kronig transitions from the L_I and L_{II} subshells. This correction factor (calculated from theoretical ionization probabilities⁹) depends on the impact parameter and varies, for the system investigated here, between 1.12 at 100 fm to 1.15 at 3000 fm. In Fig. 1 the measured photon emission probabilities $dP(b, \theta)/d\Omega$ of the L_I line per unit photon detector solid angle Ω at $\theta = 25^\circ$ and 90° polar emission angle are plot-

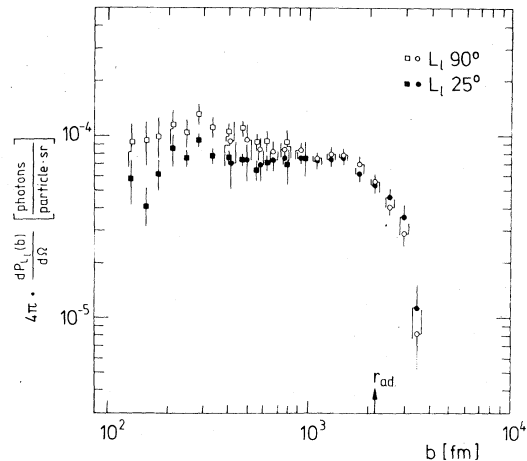


FIG. 1. Photoemission probabilities as a function of b . Squares and dots correspond to two different distances between target and particle detector.

ted versus impact parameter b . From the corrected polar anisotropy of the L_I line in coincidence with only the radial position-sensitive part of the PPAD, the values of $A_{20}(b)$ are determined by using the following relation¹⁰:

$$\frac{dP}{d\Omega}(b, \theta) = \frac{P^0(b)}{4\pi} [1 + \alpha_2 A_{20}(b) P_2(\cos\theta)], \quad (1)$$

where $P^0(b)$ is the total L_I emission probability at impact parameter b , P_2 is the Legendre polynomial of second order, and $\alpha_2 = \frac{1}{2}$ is calculated¹⁰ from the angular momenta of the $3s_{1/2}$ and $2p_{3/2}$ states. The values of $A_{20}(b)$ do not depend on the absolute values of the measured probabilities, e.g., on uncertainties in fluorescence yields, transition width, absolute solid angles, and normalizations of the probabilities. The absolute ionization probabilities will be discussed in a forthcoming paper.

The resulting A_{20} tensor component values are shown in Fig. 2 as a function of the impact parameter b . These different values of A_{20} mean a different ionization of the $|m_j| = \frac{3}{2}$ and $|m_j| = \frac{1}{2}$ magnetic substates of the L_{III} subshell; e.g., the negative A_{20} values at small b show that the ionization probability of an electron in the magnetic substate $|m_j| = \frac{1}{2}$ is larger than for one in $|m_j| = \frac{3}{2}$. This is a result which can be qualitatively understood by considering the spatial distribution of $|m_j| = \frac{3}{2}$ and $\frac{1}{2}$ $2p$ wave functions in comparison with the size of the adiabatic impact parameter $r_{ad} = \hbar v / E_B$ in this collision system (v is the projectile velocity, and E_B is the L_{III} binding energy). The transition between the positive

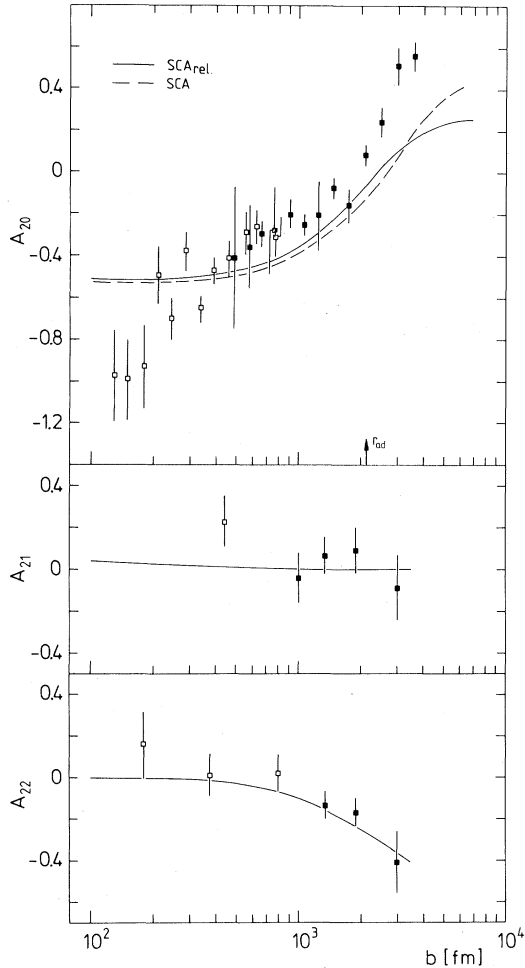


FIG. 2. A_{20} , A_{21} , and A_{22} alignment tensor components as a function of b . Open and full points correspond to two different distances between target and particle detector.

and negative regions of A_{20} occurs at about the adiabatic impact parameter, because this is the impact-parameter region where the L_{111} -shell ionization probability falls off as seen clearly in Figs. 1 and 2.

The plotted curves in Fig. 2 represent SCA calculations with relativistic hydrogenlike wave functions⁹ (solid line) and with nonrelativistic hydrogenlike wave functions¹¹ (broken line). The SCA calculations are able to reproduce the overall b dependence of the A_{20} values and are in reasonable agreement with the absolute value of A_{20} in the b range from 300 to 3500 fm. The shift towards larger impact parameter of the theoretical curve compared to the experimental data may be

due to the choice of H-like electron wave functions, as calculations with Dirac-Fock wave functions indicated.⁹ The deviations at very small b between the predictions of SCA theory and the experimental A_{20} values are not understood at present. We want to note that in an earlier experiment with the same collision system and a different experimental setup, large negative A_{20} values of the same size at b below 200 fm were also found.

The A_{22} tensor component can be determined by detection of the L_1 photons in the scattering plane ($\varphi = 90^\circ$) and use of the relation²

$$dP/d\Omega(b, \varphi) \sim 1 + \beta(b) \cos 2\varphi, \quad (2)$$

where

$$\beta(b) = 6^{1/2} \alpha_2 A_{22}(b) / [2 - \alpha_2 A_{20}(b)].$$

These A_{22} values as a function of b are displayed in Fig. 2. The values of A_{22} (and also of A_{21}) are displayed for different impact parameters than those of A_{20} , as a result of adding up rings of the PPAD in order to get smaller statistical errors. This was possible because the results before summing showed, within the error bars, only a weak dependence on b , which is also expected by the calculations (see below). In order to understand the b dependence of the A_{22} component one has to know that it is the negative product of the ionization amplitudes of the magnetic substates $m_j = +\frac{3}{2}$ and $m_j = -\frac{3}{2}$ normalized to the ionization probability of the total $2p$ subshell.¹² Therefore A_{22} should approach zero where the ionization of the $|m_j| = \frac{1}{2}$ state dominates, corresponding to a negative value of A_{20} . At large b , A_{22} should approach $-\frac{1}{2}$, where the ionization of the $|m_j| = \frac{3}{2}$ state dominates, corresponding to a positive value of A_{20} , respectively. This physical connection between A_{20} and A_{22} can be clearly seen from Fig. 2. The prediction of the SCA⁹ for $A_{22}(b)$ (solid line in Fig. 2) reproduces very well this dependence of A_{22} on b .

The A_{21} component, which is a measure of the relative phase difference between the $|m_j| = \frac{1}{2}$ and $|m_j| = \frac{3}{2}$ substate ionization amplitudes, was determined from the coincident L_1 emission probability at six different azimuthal angles φ and the four polar angles θ , by use of the following relation²:

$$dP/d\Omega(b, \theta) \sim 1 + \beta_{11}(b, \varphi) \cos[2\theta - \psi(b, \varphi)], \quad (3)$$

where

$$\beta_{11} = \frac{\alpha_2 \{ [3A_{20}(b) - 6^{1/2} A_{22}(b) \cos 2\varphi]^2 + 24A_{21}^2(b) \cos^2 \varphi \}^{1/2}}{4 + \alpha_2 [A_{20}(b) + 6^{1/2} A_{22}(b) \cos 2\varphi]}$$

and

$$\psi = \tan^{-1} \left(\frac{2 \times 6^{1/2} A_{21}(b) \cos \varphi}{3A_{20}(b) - 6^{1/2} A_{22}(b) \cos 2\varphi} \right).$$

The A_{21} values are shown in the middle part of Fig. 2. The A_{21} values show, within the error bars, no dependence on b and are consistent with an absolute value of about zero. This would mean that the relative phase difference between the amplitudes for $|m_j| = \frac{3}{2}$ and $|m_j| = \frac{1}{2}$ ionization is close to $\pi/2$. The experimental A_{21} data are in agreement with the SCA predictions⁹ (solid line), where a very weak increase to positive values with decreasing b is predicted.

From the results of this experiment we conclude that by measuring the angular distribution of photons and scattered particles by a particle-photon coincidence technique the impact-parameter-dependent A_{20} , A_{22} , and A_{21} alignment tensor components can be determined. These together with the ionization probability provide (beside being an average over the electron final states) almost complete information about the L -shell ionization in a heavy target atom. Our results show an overall agreement with first-order perturbation theory in the semiclassical approximation where the internuclear axis is used as the quantization axis. The experimental observation of nonzero A_{20} and A_{22} tensor components is a clear hint that the Coulomb field of the ionizing projectile breaks the spherical symmetry of the target atom. Besides the sensitivity to electron-correlation effects in the wave function the alignment tensor components should give access

to the dynamical behavior of electronic states by investigations at different collision velocities.

We wish to thank L. Kochbach, F. Rösel, and D. Trautmann for making their calculations available to us. This work is supported by the Bundesministerium für Forschung und Technologie.

¹W. Mehlhorn, in *X-Ray and Atomic Inner Shell Physics—1982*, edited by B. Crasemann, AIP Conference Proceedings No. 94 (American Institute of Physics, New York, 1982), p. 53.

²E. G. Berezhko, N. M. Kabachnik, and V. V. Sizov, *J. Phys. B* **11**, 1819 (1978).

³W. Jitschin, H. Kleinpoppen, R. Hippler, and H. O. Lutz, *J. Phys. B* **12**, 4077 (1979).

⁴J. Palinkás, L. Sarkardi, and B. Schlenk, *J. Phys. B* **13**, 3829 (1980).

⁵G. Richter, M. Brüssermann, S. Ost, J. Wigger, C. Cleff, and R. Santo, *Phys. Lett.* **82A**, 412 (1981).

⁶E. C. Sewell and A. Crowe, *J. Phys. B* **15**, L357 (1982).

⁷G. Gaukler, H. Schmidt-Böcking, R. Schuch, R. Schule, H. J. Specht, and I. Tserruya, *Nucl. Instrum. Methods* **141**, 115 (1977).

⁸R. Hoffmann, G. Gaukler, G. Nolte, H. Schmidt-Böcking, and R. Schuch, *Nucl. Instrum. Methods* **197**, 391 (1982).

⁹F. Rösel, D. Trautmann, and R. Baur, *Z. Phys. A* **304**, 75 (1982), and private communication.

¹⁰E. G. Berezhko and N. M. Kabachnik, *J. Phys. B* **10**, 2467 (1977).

¹¹L. Kochbach, J. M. Hansteen, and R. Gundersen, *Phys. Scr.* **27**, 54 (1983).

¹²F. J. Paixão, N. T. Padial, Gy. Csanak, and K. Blum, *Phys. Rev. Lett.* **45**, 1164 (1980).